Surface & Coatings Technology 400 (2020) 126216

Contents lists available at ScienceDirect

Surface & Coatings Technology

journal homepage: www.elsevier.com/locate/surfcoat

Antimicrobial modification of PLA scaffolds with ascorbic and fumaric acids via plasma treatment

Anton Popelka[a,*], Asma Abdulkareem[a], Abdelrahman A. Mahmoud[b], Mohammed G. Nassr[b], Mahmoud Khatib A.A. Al-Ruweidi[b], Khalid J. Mohamoud[b], Mohammed K. Hussein[b], Marian Lehocky[c,d], Daniela Vesela[c], Petr Humpolíček[c,d], Peter Kasak[a]

[a] Center for Advanced Materials, Qatar University, P.O. Box 2713, Doha, Qatar
[b] Department of Chemistry and Earth Sciences, Qatar University, P.O. Box 2713, Doha, Qatar
[c] Centre of Polymer Systems, Tomas Bata University in Zlin, Trida Tomase Bati 5678, 760 01 Zlin, Czech Republic
[d] Faculty of Technology, Tomas Bata University in Zlin, Vavreckova 275, 760 01 Zlin, Czech Republic

ARTICLE INFO

Keywords:
PLA
Plasma treatment
Surface modification
Ascorbic acid
Fumaric acid

ABSTRACT

An optimal medical scaffold should be biocompatible and biodegradable and should have adequate mechanical properties and scaffold architecture porosity, a precise three-dimensional shape, and a reasonable manufacturing method. Polylactic acid (PLA) is a natural biodegradable thermoplastic aliphatic polyester that can be fabricated into nanofiber structures through many techniques, and electrospinning is one of the most widely used methods. Medical fiber mat scaffolds have been associated with inflammation and infection and, in some cases, have resulted in tissue degradation. Therefore, surface modification with antimicrobial agents represents a suitable solution if the mechanical properties of the fiber mats are not affected. In this study, the surfaces of electrospun PLA fiber mats were modified with naturally occurring L-ascorbic acid (ASA) or fumaric acid (FA) via a plasma treatment method. It was found that 30 s of radio-frequency (RF) plasma treatment was effective enough for the wettability enhancement and hydroperoxide formation needed for subsequent grafting reactions with antimicrobial agents upon their decomposition. This modification led to changes in the surface properties of the PLA fiber mats, which were analyzed by various spectroscopic and microscopic techniques. FTIR-ATR confirmed the chemical composition changes after the modification process and the surface morphology/topography changes were proven by SEM and AFM. Moreover, nanomechanical changes of prepared PLA fiber mats were investigated by AFM using amplitude modulation-frequency modulation (AM-FM) technique. A significant enhancement in antimicrobial activity of such modified PLA fiber mats against gram-positive *Staphylococcus aureus* and gram-negative *Escherichia coli* are demonstrated herein.

1. Introduction

Surgical procedures are routinely performed for the repair and/or replacement of damaged tissue caused by disease or trauma. Designing biomaterial scaffolds with porous structures is crucial for tissue engineering applications. The most important factors that enable the use of these materials in tissue engineering are biocompatibility, mechanical properties, required manufacturing technology, biodegradability and scaffold architecture [1]. Scaffolds must imitate the functional and mechanical properties of the extracellular matrix of the tissue to be repaired [2]. Various polymeric materials utilizing 3D porous structures have been applied in scaffold fabrication; these materials include polyurethane, poly-ε-caprolactone, polytetrafluoroethylene, polyethylene glycol hydrogels, and polylactic acid (PLA) [3]. These materials have adequate mechanical properties and show low infection susceptibility after their in vivo degradation [4–6]. However, many of these materials have been abandoned because local reactions with tissues increase the risk of meningitis symptoms, excessive scar formation or hemorrhage [7–9].

Electrospinning is one of the most commonly used techniques for the fabrication of scaffolds because the final parameters (fiber dimensions, morphology and porosity) can be easily controlled, and the large specific surface areas required for tissue reconstruction can be obtained [10–14]. Scaffolds fabricated using electrospinning based on PLA fibers have excellent mechanical properties that are similar to natural tissues [15]. Moreover, this polymeric material is rapidly degraded. However,

* Corresponding author.
E-mail address: anton.popelka@qu.edu.qa (A. Popelka).

https://doi.org/10.1016/j.surfcoat.2020.126216
Received 20 May 2020; Received in revised form 12 July 2020; Accepted 17 July 2020
Available online 21 July 2020

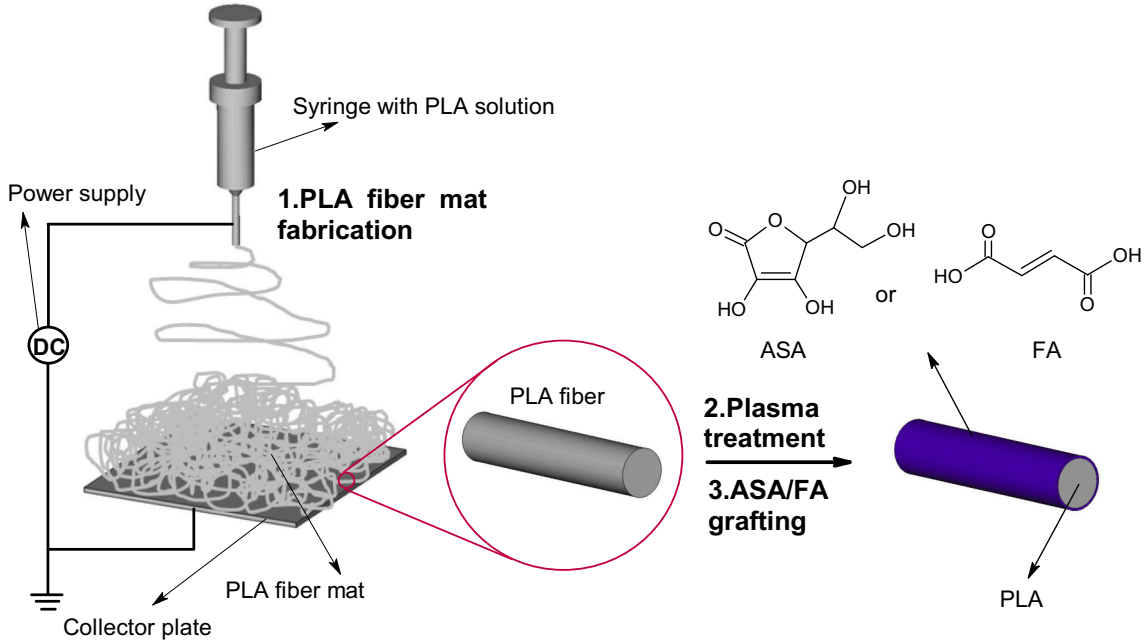

Fig. 1. Preparation of antimicrobial PLA nanofibers mats: 1. electrospinning of PLA solution, 2. plasma treatment, 3. radical grafting of ASA or FA.

its low surface free energy (wettability) gives rise to weak adhesion properties and low cell proliferation [16].

Low-temperature plasma technology is a modification technique applicable in tissue engineering applications that allows the incorporation of new functionalities into the scaffold surface and can improve wettability. Plasma treatment can initiate the formation of radicals necessary for subsequent grafting reactions and can covalently bond additional functionalities onto the treated surface [17–19]. Plasma treatment has been applied on PLA films to improve cell attachment but did not show marked differences after seven days of cultivation [20]. Cell adhesion was shown to improve by grafting acrylic acid onto electrospun PLA fiber mats through plasma treatment [21]. Many studies related to the surface treatment and modification of PLA fibers were reported but mainly focused on the cell adhesion and growth enhancement with lacking information about their antimicrobial activity [22,23].

The major problem of using scaffolds in tissue engineering is their susceptibility to infection as a result of bacteria colonization and subsequent proliferation, resulting in biofilm formation [24,25]. Various bacterial pathogens such as *Staphylococci* and *Streptococci* are responsible for serious infections in wound sites, and these bacteria are often present on the skin [26]. For this reason, the design of advanced scaffolds with antimicrobial actively is highly anticipated.

The surface modification of PLA scaffolds has shown acceptable production parameters in terms of effectiveness, cost and the time required. In our study, ascorbic acid (ASA) and fumaric acid (FA) were selected as promising naturally abundant materials for antimicrobial modification because of their nontoxicity, biocompatibility and antimicrobial effect [27,28]. Only the top surface layer of the modified scaffold is effective for killing bacteria because it is in direct contact with the organism. Thus, such modifications do not affect the bulk mechanical properties of the scaffold. There are several studies related to the surface modification of PLA, which led to the significant improvement in the antimicrobial activity [29–31]. However, they were mainly realized in the film form or using expensive noble metals as the antimicrobial agents. The another study was focused on the PLA nonwoven fibers modified with fosfomycin by a simply impregnation process, which proved the inhibition zones of the bacterial growth as the antimicrobial agent was released from the modified PLA fibers [32].

The surface modification of PLA electrospun fiber mats with covalently bonded ASA or FA through plasma treatment was performed for the first time by our knowledge and this study provides complex approach for the preparation of antimicrobial surfaces applicable in medicinal polymeric oriented applications.

2. Experimental

2.1. Materials

The following materials were used to produce the electrospun fiber mats: polylactic acid (PLA): Ingeo 2002D with a D-isomer content of 4.3%, MW of 2.53×10^5 g/mol, melt flow index of 6 g/10 min (190 °C/2.16 kg), and density of 1.24 g/cm^3 (NatureWorks, USA); *N*,*N*-dimethylformamide (DMF): anhydrous (≥99.9% purity), inhibitor-free (Sigma-Aldrich, USA); and dichloromethane (DCM): anhydrous (≥99% purity), inhibitor-free (BDH, UK). Ethylene glycol (> 98% FLUKA, Belgium), formamide (> 98% FLUKA) and ultra-pure water (prepared by Purification System Direct Q3, France) were used as testing liquids for the wettability analysis. Fumaric acid (FA): $C_4H_4O_4$, MW: 116.07 g/mol (Merck KGaA, Germany) and L-ascorbic acid (ASA): (vitamin C), $C_6H_8O_6$, MW: 176.13 g/mol (Research-lab Fine Chem Industries (RLFCI), India) were used as antimicrobial agents. Sodium iodide: extra pure, MW: 197.89 g/mol (RLFCI); glacial acetic acid (CH_3COOH): (VWR International (BDH) Chemicals, USA) anhydrous (≥99.9% purity); and sodium thiosulfate pentahydrate $Na_2S_2O_3{\cdot}5H_2O$: extra pure, MW 248.17 g/mol, (RLFCI) were used for the iodometric titration.

2.2. Sample preparation

The main objective was to modify the PLA scaffold surface with antimicrobial agents that were biodegradable, naturally occurring, highly abundant, nontoxic and cost-effective using a mild technique to promote surface adhesion without negatively impacting the mechanical properties of the scaffold. The PLA fiber mats were prepared using an electrospinning technique (Fig. 1, step 1.) that ensured a large surface area. Next, the surface of the PLA fibers was modified by plasma-assisted grafting (Fig. 1, step 2.). Finally, the plasma-treated fibers were mixed with the antimicrobial agents ASA (vitamin C) [33] or FA (a component of aloe) [34] (Fig. 1, step 3.), as depicted in Fig. 1.

To produce the PLA fibers, electrospinning was carried out with a

Table 1
Surface morphology and structural properties of the PLA fiber mats.

PLA (%)	Structure	Mean fiber diameter (nm)	Ra (nm)	WCA (°)
3	Beading fibers	152.2 ± 15.9	238.2	115.2 ± 2.7
5	Beading fibers	314.1 ± 46.7	385.1	132.2 ± 1.7
7	Defect-free	1256.6 ± 136.9	975.4	116.0 ± 3.5
10	Defect-free	343.2 ± 57.1	192.3	102.7 ± 7.9
12	Defect-free	948.4 ± 124.9	901.4	115.0 ± 6.6
15	No fibers	N.A.	N.A.	N.A.

NaBond (China) electrospinning device. Aluminum foil placed on the rotating drum was used to collect the fibers to ensure an electrically conductive substrate. For the electrospinning process, solutions of different concentrations of PLA in a binary solvent of DCM/DMF (70:30) was fed into a 10 mL plastic syringe, and the flow rate was controlled at 2.5 mL/h by a syringe pump. A silicon tube was used to connect the syringe, and a conductive needle was connected to a high-voltage electrical circuit. The needle was set up vertically, and the distance between the needle tip and the collector covered with aluminum foil was adjusted to approximately 15 cm. The voltage applied to the needle was 12 kV. The resulting fibers were collected on the aluminum foil and used in subsequent characterizations.

2.3. Plasma treatment

Low-temperature plasma treatment of the PLA fiber mats was carried out under vacuum using the Venus75-HF plasma system (Plasma Etch Inc., Carson, USA). During the plasma treatment, ions and electrons were generated by means of radio-frequency (RF) nominal power at a frequency of 13.56 MHz. The treatment time was varied to optimize the plasma treatment process and to obtain the maximum wettability and hydroperoxide concentration. The chamber was evacuated to a vacuum level of 27 Pa, and the treatment was applied from 10 s up to 180 s at 80 W of nominal power. The samples were treated from both sides.

2.4. Surface modification by antimicrobial agents

Grafting was carried out for 24 h on fresh plasma-treated PLA fiber samples immersed in 10% ASA (w/v) aqueous solution or in 5% FA (w/v) ethanol solution.

The samples were then thoroughly washed and dried. Graft yield measurements were conducted on three different samples to verify the grafting of ASA or FA onto the PLA surface. The gravimetric measurements were used to calculate graft yield of modified PLA. The graft yield (GY) was calculated by Eq. (1):

$$GY\ [\%] = ((W_2 - W_1)/W_1).100\% \quad (1)$$

where W_1 and W_2 represent the weights of the PLA samples before and after the modification.

2.5. Wettability analysis

Changes in the wettability of the PLA fiber mats treated with plasma and modified by antimicrobial agents were evaluated using static water contact angle measurements. An optical contact angle measuring system OCA35 (DataPhysics, Germany) was used in this study and was equipped with a high-resolution CCD camera. Ultra-pure water, ethylene glycol and formamide were used as testing liquids. A water droplet of approximately 1 μL was dispensed onto the sample in ambient air to eliminate gravitational effects. Five independent measurements in different positions were carried out, and the average contact angle was obtained. The total surface free energy and its polar and dispersive

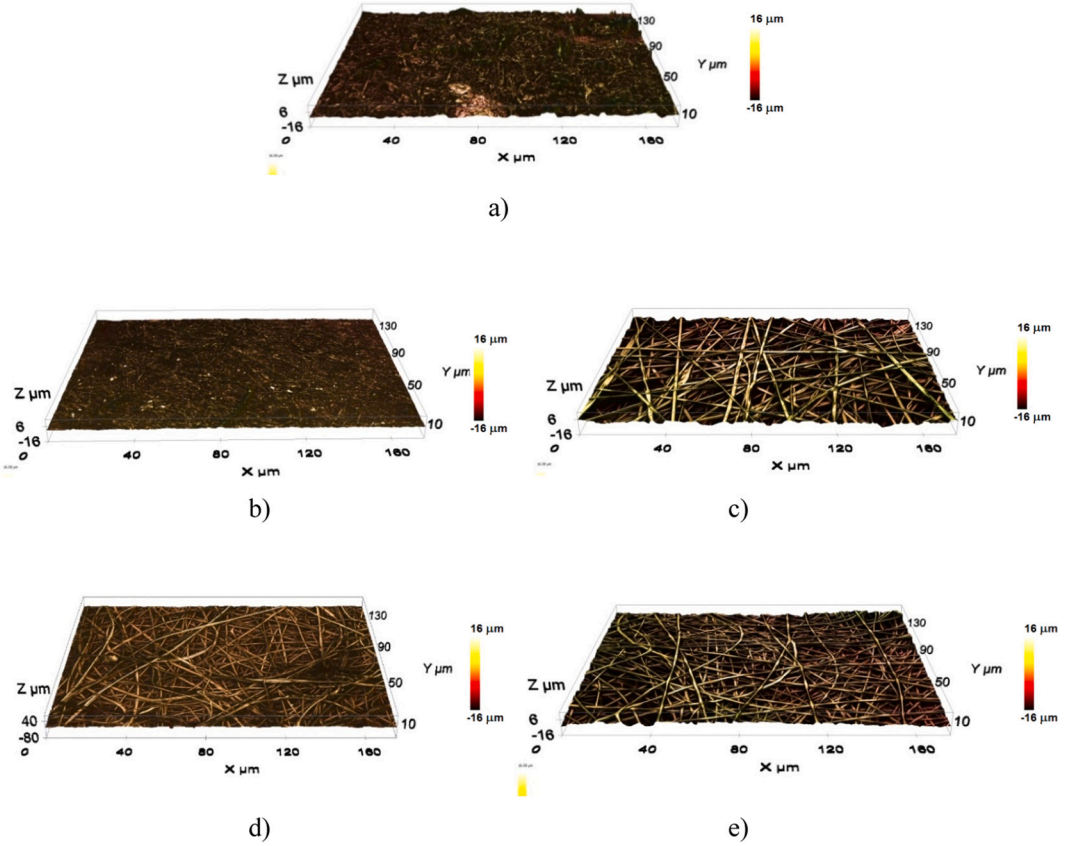

Fig. 2. Profilometry images of PLA fiber mats: a) 3%, b) 5%, c) 7%, d) 10%, e) 12%.

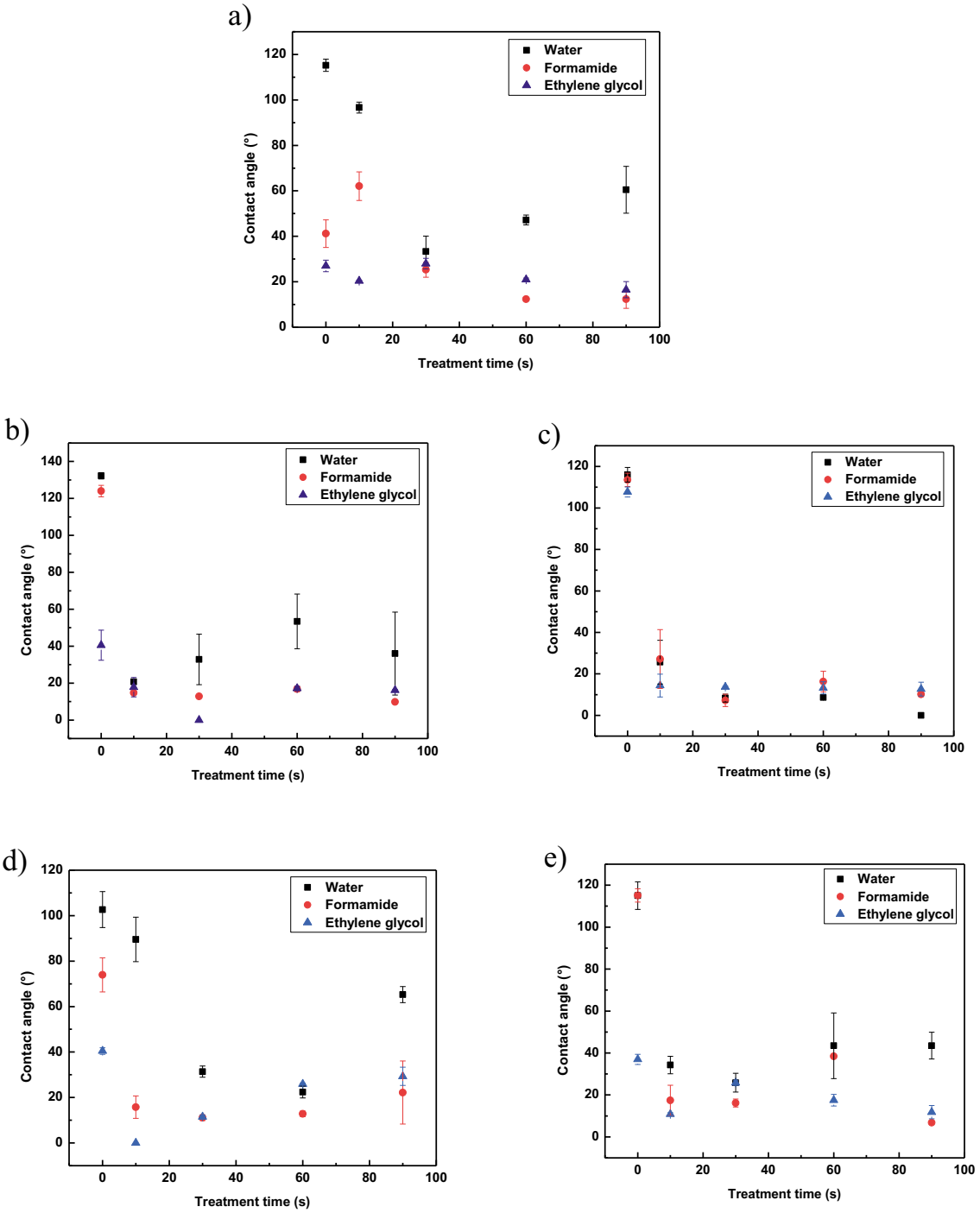

Fig. 3. Changes in contact angle of plasma-treated PLA electrospun fibers: a) 3%, b) 5%, c) 7%, d) 10%, e) 12%.

components were evaluated using the Owens, Wendt, Rabel, Kaelble model.

2.6. Hydroperoxide determination

The modified iodometric method based on Wagner et al. [35] was applied to quantitatively detect the hydroperoxides created on the PLA surface after plasma treatment. This method involves the following reactions. The first reaction is the combination of acetic acid, sodium iodide and hydroperoxide ($1H_2O_2$:$1I_2$) Eq. (2):

$$H_2O_2 + 2NaI + 2CH_3COOH \rightarrow 2CH_3COONa + I_2 + 2H_2O \quad (2)$$

The next reactions involve molecular iodine I_2 reacting with thiosulfate to measure the hydroperoxide concentration through the quantity of iodine reduced ($1I_2$:$2I^-$) Eq. (3) and Eq. (4):

$$Na_2S_2O_3 + H_2O \rightarrow S_2O_3^{2-} + Na^+ + H^+ + OH^- \quad (3)$$

$$2S_2O_3^{2-} + I_2 \rightarrow S_4O_6^{2-} + 2I^- \quad (4)$$

PLA samples were placed inside an Erlenmeyer flask containing 50 mL of glacial acetic acid and 1 g of sodium iodide. The flask was covered with aluminum foil due to the light sensitivity of sodium iodide. The reactions were carried out under an inert argon atmosphere and in the dark to ensure iodide oxidation only by hydroperoxides. After iodide oxidation to iodine, the mixture turned yellow. The subsequent titration with sodium thiosulfate solution (0.0005 M) resulted

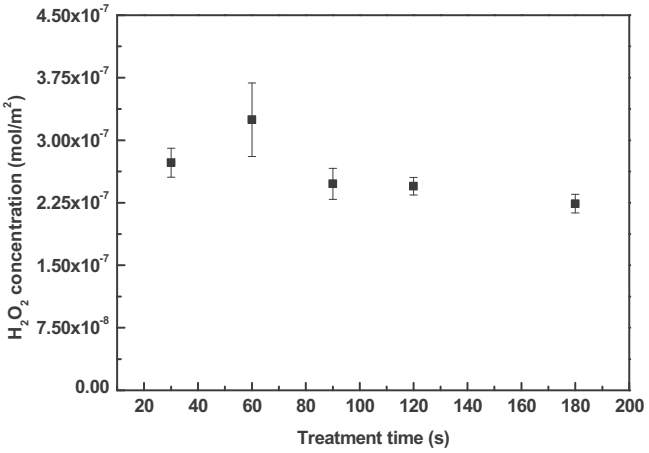

Fig. 4. Hydroperoxide concentration of plasma treated PLA fiber mats vs. treatment time.

in a colorless solution after reaching the titration threshold, and the concentration of hydroperoxide per treated area was calculated.

2.7. Surface morphology analysis

The surface topography of untreated, plasma-treated and anti-microbial-modified PLA electrospun fiber mats was analyzed using an optical surface metrology confocal system profilometer (Leica DCM8; Leica Microsystems, Germany). The optical system was used for high-accuracy surface profiling to optimize the PLA fiber mat formation. Images of 175 × 132 μm^2 were captured using an EPI 100 × 0.9-L objective lens.

The surface morphology of untreated, plasma-treated and anti-microbial-modified electrospun PLA fiber mats was studied using scanning electron microscopy (SEM). A NanoSEM 450 microscope (FEI, USA) was used to obtain 2D images of the analyzed surfaces. To obtain high-resolution SEM images, thin Au layers (a few nanometers thick) were sputter-coated onto the PLA samples to prevent the accumulation of electrons in the measured layer.

The surface topography of the untreated, plasma-treated and anti-microbial-modified electrospun PLA fiber mats was analyzed by atomic force microscopy (AFM) using an MFP-3D system (Asylum Research, USA) equipped with an AC160TS cantilever (Al reflex-coated Veeco model-OLTESPA, Olympus, Japan). Scanning was carried out under ambient conditions using tapping mode in air (AC mode) over 20 × 20 μm^2 and 5 × 5 μm^2 surface areas. In addition, the roughness parameter (Ra) representing the arithmetic average of the roughness profile was evaluated from the obtained AFM z-sensor images.

2.8. Mechanical properties characterization

AFM was also used to determine the mechanical properties of the PLA samples using the amplitude modulation-frequency modulation (AM-FM) mode. This technique is an extension of standard AC mode (also known as AM-AFM) in which the probe is excited simultaneously at its fundamental resonant frequency and at another eigenmode. The

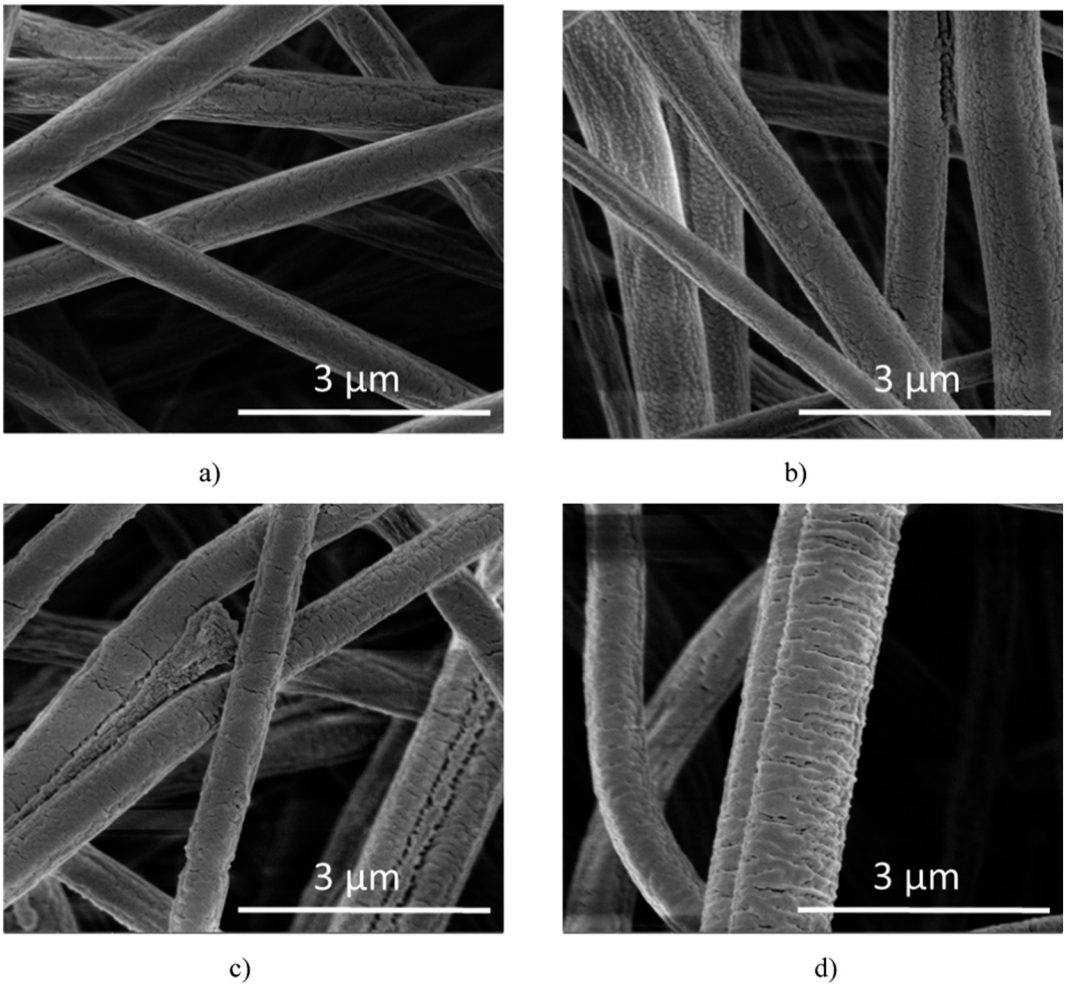

Fig. 5. Detailed SEM images of 10% PLA fiber mats: a) untreated, b) plasma treated, c) ASA grafted, d) FA grafted.

fundamental resonance was employed to determine the topographical features of the electrospun PLA fiber mats, whereas the mechanical properties were analyzed by tracking the frequency and amplitude shift of the other eigenmode. The measured frequency shift Δf was then used to estimate the interaction stiffness (Δk^{FM}) by Eq. (5):

$$\Delta k^{FM} \approx 2k_c . \Delta f/f_c \quad (5)$$

where k_c is the spring constant of the cantilever and f_c is the frequency of the eigenmode of the cantilever. To obtain the Young's modulus of the sample, a general Hertz model was applied, which described the contact mechanics between the tip and analyzed sample. A standard electrospun PLA fiber mat with a known Young's modulus (632.3 MPa) was first used to calibrate the cantilever and determine its elasticity. This elasticity was then used to obtain the absolute values of Young's modulus of the analyzed samples.

2.9. Chemical composition analyses

The functional groups and chemical structure composition changes in the plasma-treated and modified PLA fiber mats were analyzed by Fourier transform infrared spectroscopy with attenuated accessory (FTIR-ATR). A Spectrum 400 (Perkin Elmer, USA) was used to identify the functional groups introduced after the plasma treatment and the antimicrobial agent modifications on the PLA fiber mats. All measurements were obtained through 8 scans with a resolution of 4 after background subtraction in the middle infrared region (4000–700 cm^{-1}).

2.10. Antimicrobial tests

A modified version of an internationally recognized test method to evaluate the antibacterial activity of modified plastic materials (ISO 22196) was used to investigate the antimicrobial effect of the prepared samples [36]. First, all samples were disinfected by UV radiation and then placed in sterile Petri dishes. Samples with dimensions of 25 × 25 mm^2 were then inoculated using a standardized bacteria suspension of *Staphylococcus aureus* (*S. aureus*) (CCM 4516 – $3.9.10^5$ cfu/mL) and *Escherichia coli* (*E. coli*) (CCM 4517 – $1.2.10^7$ cfu/mL), and the samples were covered with ethanol-disinfected polypropylene foil with dimensions of 20 × 20 mm^2. The inoculated samples were incubated at 95% relative humidity and 35 °C for 24 h. The polypropylene foil was then removed from the samples, which were subsequently imprinted on agar (3 times on different areas), and the agar was incubated at 35 °C for 24 h. The number of bacterial colonies was evaluated on a scale of 0–5, where 0 represented the best antimicrobial effect, i.e., without bacterial growth. An additional incubation at 35 °C for 24 h was performed, followed by the final colony evaluation.

3. Results and discussion

3.1. Optimization of the fiber mat fabrication

Information regarding the 2D surface morphology of the prepared PLA fiber mats obtained by SEM is summarized in Fig. S1, Supporting Information. Profilometry and SEM was used to analyze the electrospinning process for the different concentrations of PLA solution. Prior to measurement, the PLA fiber mat samples were coated with a thin layer of gold that was a few nanometers thick. This was applied mainly to obtain higher resolution images for profilometry and to prevent the accumulation of electrons in the measured layer from causing a brightening effect in the SEM. SEM was also used to determine the fiber diameter, and the results are summarized in Table 1 including information about water contact angle (WCA) and Ra (roughness parameter). The differences in concentrations of PLA solutions affected the resulting fibers structures and therefore also their wettability. The 3% PLA solution resulted in thin fibers that contained thick bead-shaped structures. An increased amount of bead formation was associated with lower concentrations of the PLA solution (Fig. S1a, Supporting Information). The 5% PLA solution (Fig. S1b, Supporting Information) resulted in less bead formation in the fiber mats but gave larger diameter fibers. Fig. S1c, Supporting Information, shows the PLA fiber mats prepared with 7% PLA solution; these consisted of smooth defect-free fibers but had large diameters (1256.6 ± 136.9 nm). The 10% PLA solution gave smooth, thin, and defect-free PLA fiber mats (Fig. S1d, Supporting Information); these fibers had a diameter of 343.2 ± 57.1 nm. The application of 12% PLA solution in the electrospinning led to the formation of defect-free fiber mats but with larger diameters (948.4 ± 124.9 nm) (Fig. S1e, Supporting Information). The high-concentration PLA solution (15%) resulted in stacking in the needle and therefore it could not undergo electrospinning. The diameters of the fabricated fibers were in agreement with those of previous studies [37]. The surface morphology, particularly the surface roughness, affected the wettability of the PLA fiber mats. The thicker defect-free fibers gave rise to lower wettability and vice versa. A trapped air between PLA fibers with larger Ra values was probably responsible for higher WCA according to the Cassie–Baxter regime [38]. The bead-containing fibers generate higher WCA than bead free-containing fibers [39]. This is mainly caused by rougher beading structures in compare with only fiber ones [40]. Many studies showed that the fiber diameter decrease led to the increase of WCA [41–43]. However, the smallest fibers contained also beading structures or relatively large pore size between fibers (more than 2.1 μm). In contrary, some other studies confirmed the increase of WCA with the fibers diameter increase [44,45]. Therefore, the surface roughness analyses are necessary for the correct interpretation of wettability of the electrospun fibers [46].

The surface topography of the electrospun PLA fiber mats was investigated using the optical surface metrology profilometry system over a relatively large surface area (175.31 × 131.97 μm^2). Images of the electrospun PLA fiber mats prepared from different PLA concentrations (3%–12%) are shown in Fig. 2. The mats prepared from lower concentrations (3% and 5%) resulted in the formation of small fibers, but the fibers included bead structures. Increasing the PLA concentration to 7% led to defect-free fiber mats but with relatively large fiber diameters. Increasing the PLA concentration to 10% gave defect-free fiber mats with the finest structures. The 12% solution of PLA resulted in the formation of regular defect-free fiber mats but with larger fiber diameters. The contact angles of the fiber mats ranged from 102° for the 10% PLA to 132° for 5% PLA samples (Table 1). The micro-nano structural architecture formed through a combination of beads and fibers, as well as higher diameter fibers, resulted in greater hydrophobicity of the fiber mats.

The 3D surface topography of the prepared PLA fiber mats was analyzed by AFM. Images of the fiber mats prepared using PLA solutions with different concentrations were obtained from the 20 × 20 μm^2 surface area (Fig. S2, Supporting Information). The AFM images clearly show an increase of fiber diameter with increasing PLA concentration (up to 7%). The 10% PLA solution resulted in fiber mats with excellent regular structure and fibers with smaller diameters. Further increasing the PLA concentration again led to the formation of thicker fibers. These findings closely correspond to the SEM analyses. AFM was also used to evaluate the surface roughness parameter (Ra), which represents the height of irregularities perpendicular to the surface. The Ra value of the PLA fiber mats prepared at the lowest concentration (3%) was 238.2 nm. The Ra value increased with increasing PLA solution concentration up to 7%, achieving 975.4 nm. The 10% PLA solution resulted in fiber mats with the thinnest structures and an Ra value of 192.3 nm evaluated over a 20 × 20 μm^2 area. Further increasing the PLA solution concentration (12%) resulted in thicker fibers and an Ra value of 901.4 nm. The PLA fiber mats prepared from 10% solution were therefore selected as the optimal samples for subsequent plasma treatment and modification by ASA or FA.

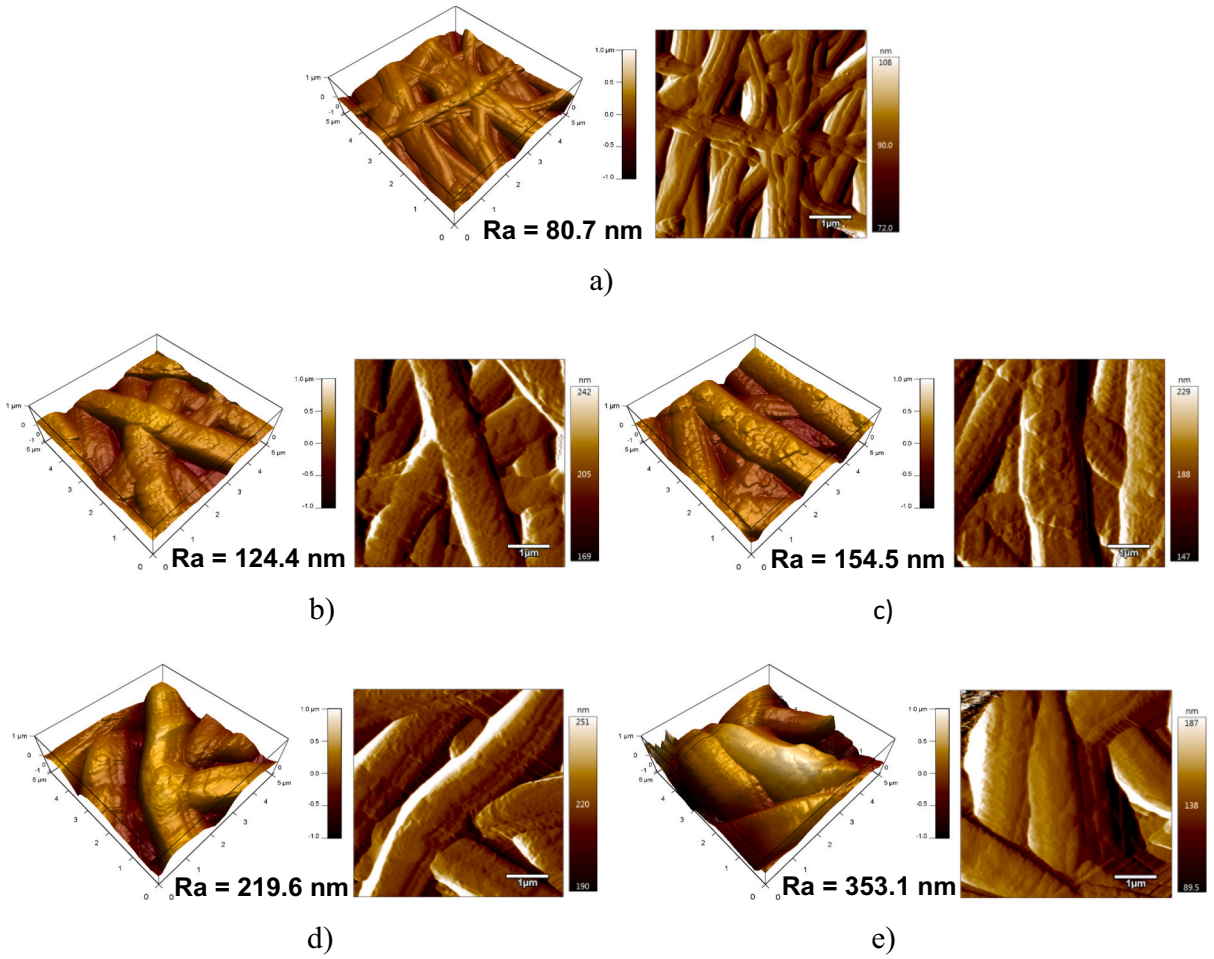

Fig. 6. Detailed AFM images of 10% PLA fiber mats: a) untreated, b) plasma treated 30 s, c) plasma treated 60 s, d) ASA grafted, e) FA grafted.

3.2. Plasma treatment optimization

Contact angle measurements were performed to analyze the effect of plasma treatment on the wettability of the prepared electrospun PLA fiber mats (Fig. 3). Water, which has a relatively high surface tension of ~72.1 mN/m, showed relatively high values of WCA greater than 100°. By contrast, liquids with relatively low surface tensions, such as ethylene glycol (~48.0 mN/m) and formamide (~58.2 mN/m), showed low contact angles on untreated PLA fiber mats compared with water. Plasma treatment of the PLA fiber mats improved the wettability [47], which was confirmed by the decreased contact angles, as result of incorporating new functionalities, etching, and ablation [48]. The decrease in contact angles after plasma treatment can be described by Wenzel wetting theory [49], while the pores can be wetted too. The lowest values of contact angles after plasma treatment were observed for the defect-free PLA fiber mats with the highest surface roughness. WCA was decreasing with increasing plasma treatment time up to 30 s for the all PLA samples except 5% of PLA, where WCA achieved minimum after 10 s of plasma treatment. An additional increase in treatment time led to slightly decrease of WCA or gave rise to higher water contact angles depending on the PLA sample. Therefore, 30 s of RF plasma treatment resulted in a sufficient wettability improvement for all prepared PLA fiber mats, while WCA of 10% PLA achieved value 31.4°. This was noticeable less in compare with other study, in which 30 s of RF oxygen plasma treatment of PLA fiber mats resulted to 75.1° of WCA [21].

Iodometric titration was used to determine the concentration of hydroperoxide present on the PLA surface after plasma treatment,

Table 2
Surface properties of 10% PLA fiber mats.

Sample	Θ_W (°)	Θ_{FM} (°)	Θ_{EG} (°)	γ^{Total} (mJ/m^2)	γ^d (mJ/m^2)	γ^p (mJ/m^2)	GY (%)
Untreated	102.7 (± 7.9)	74.0 (± 7.5)	40.5 (± 1.4)	100.1	93.9	6.2	–
Plasma treated	31.4 (± 2.5)	11.1 (± 1.2)	11.5 (± 0.8)	72.1	4.6	67.5	–
ASA grafted	27.5 (± 0.3)	9.3 (± 5.4)	15.9 (± 2.7)	70.0	4.4	65.6	31.8 (± 11.4)
FA grafted	117.5 (± 1.6)	0 (± 0)	0 (± 0)	–	–	–	17.1 (± 9.8)

W - water, FM - formamide, EG - ethylene glycol, γ^{Total} - total surface free energy, γ^d - dispersive component of surface free energy, γ^p - polar component of surface free energy, GY - graft yield.

which is necessary for the ASA or FA grafting reactions in which they decompose into alkoxy radicals [50,51]. ASA is a water-soluble free radical scavenger [37,38] and can form ascorbate radicals by electron transfer to the created alkoxy radical, which can then react with other radicals or double bonds formed during plasma treatment. FA contains labile double bonds in its chemical structure; these are able to directly react with the formed alkoxy radicals. The quantitative analysis was performed by iodometric titration. The results of the iodometric titration of the plasma-treated PLA samples using different treatment times are summarized in Fig. 4. Plasma treatment was carried out different lengths of time. Plasma treatment for 30 s resulted in hydroperoxide concentrations of 2.7 × 10^{-7} mol/m^2. Plasma treatment for 60 s increased the hydroperoxide concentration to 3.24 × 10^{-7} mol/m^2. The additional increase of treatment time led to decreasing hydroperoxide concentrations. The hydroperoxide concentration was the highest after 60 s. However, longer plasma treatment times can result in degradation processes (see the AFM section); therefore, 30 s of plasma treatment was chosen for subsequent modification by antimicrobial agents.

3.3. Surface morphology/topography

The surface morphology changes of the plasma-treated and modified PLA fiber mats are shown in Fig. 5. The SEM image of untreated PLA (Fig. 5a) exhibited regular structures of individual fibers with a characteristic texture that originated from the electrospinning process. Plasma treatment increased the roughness as a result of etching, ablation and degradation processes (Fig. 5b). The PLA fiber mats modified by ASA (Fig. 5c) or FA (Fig. 5d) revealed specific textures on the fibers surfaces, confirming that the fibers were coated after the modification process.

Detailed AFM images were obtained from 5 × 5 μm^2 surface areas to analyze the effect of plasma treatment and subsequent modification by antimicrobial agents on the surface topography/morphology (Fig. 6). The untreated PLA fibers revealed relatively smooth structures with an Ra of 80.7 nm. Plasma treatment led to a marked increase in surface roughness. The 30 s plasma treatment time increased the surface roughness, and the Ra increased to 124.4 nm. The additional increase of plasma treatment time to 60 s led to rougher fiber surfaces, and the fibers showed many bulges; these were associated with the presence of low molecular weight oxidative products caused by polymer chain scission processes [52]. The Ra value for this sample was 154.5 nm. The modification of PLA by ASA or FA led to a smoother surface coating for a portion of the fibers. However, the antimicrobial coating increased the overall roughness; the Ra values were 219.6 and 353.1 nm for ASA and FA, respectively. The surface properties related to wettability and GY of 10% PLA fiber mats are summarized in Table 2. As was discussed earlier, plasma treatment led to the significant enhancement of wettability, while WCA, contact angle of formamide and ethylene glycol decreased from 102.7°, 74.0° and 40.5° to 31.4°, 11.1°, and 11.5°, respectively, and therefore γ^P increased from 6.2 mJ/m^2 to 67.5 mJ/m^2. The modification of the PLA fiber mats by ASA led to the additional decrease of WCA and formamide to 27.5° and 9.3°, respectively, while the contact angle of ethylene glycol slightly increased to 15.9° in compare with plasma treated samples, while γ^P was 65.6 mJ/m^2. The modification of the PLA fiber mats by FA led to the significant increase of WCA to 117°, while the samples were totally wetted by formamide and ethylene glycol and therefore γ^P could not be evaluated. The high WCA was probably associated with water resistivity of FA [53]. The GY analyses proved the presence of ASA and FA on the PLA fiber mats as the result of the combination of chemical and physical bonding, while almost double GY was observed for the modification by ASA in compare with FA.

3.4. Chemical composition analyses

The FTIR-ATR results show the chemical changes after each modification step (Fig. 7). The FTIR-ATR spectrum of untreated PLA consisted of characteristic absorption bands (Fig. 7a) [54]. The FTIR-ATR spectrum of PLA after plasma treatment revealed slight changes in the intensities of the absorption bands associated with oxygen-containing groups (Fig. 7b). The important FTIR-ATR regions of the plasma-treated PLA show new absorption bands at a maximum wavenumber of 1823 cm^{-1}, which probably belongs to two C═O stretching vibrations for anhydrides, together with adsorption bands at 1750 cm^{-1} [55] and 1620 cm^{-1}, with are potentially overlapped by C═C vibrations. Moreover, plasma treatment led to the presence of –OH-associated absorption bands in the wavenumber region 3300 to 3500 cm^{-1}. The appearance of such peaks indicates the introduction of carbonyl-, carboxyl- and hydroxyl-based functional groups, which is in agreement with previous observations and studies and demonstrates suitable functionality for grafting [56].

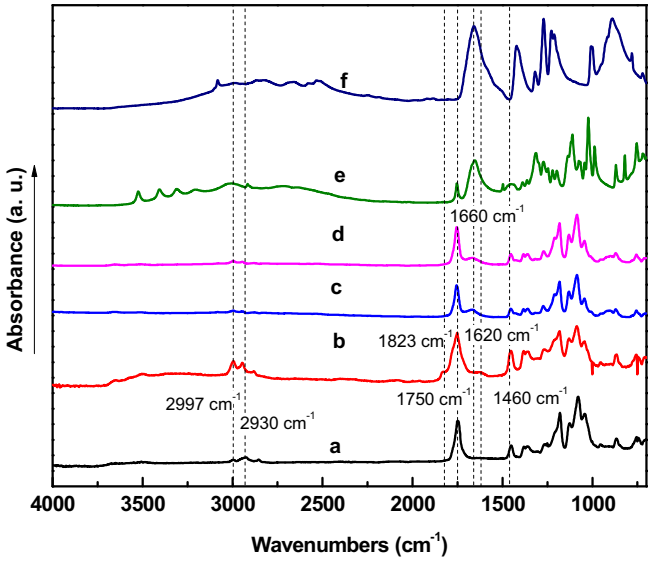

Fig. 7. FTIR-ATR spectra of 10% PLA fiber mats: a) untreated, b) plasma treated, c) ASA grafted, d) FA grafted; e) neat ASA, f) neat FA.

The FTIR spectra of PLA fiber mats modified by ASA or FA are shown in Fig. 7c,d. There is a peak shift at 1660 cm^{-1} associated with C═O stretching that clearly indicates the grafting of ASA or FA; these peaks are also observed in their pure form (Fig. 7e,f). Additionally, there were decreased intensities of the absorption bands at 2997 cm^{-1} and 2930 cm^{-1} (attributed to -CH stretching) and of 1460 cm^{-1} (attributed to -CH in-plane bending), indicating grafting of the agents onto the PLA chain. The absorption peak at approximately 3500 cm^{-1} is ascribed to -OH stretching vibration. These observations confirmed the successful grafting of both agents onto the PLA fibers, forming a coat of antimicrobial agent. We believe that the grafting is enabled through a combination of chemical and physical bonding of the antimicrobial agent to the PLA scaffold.

3.5. Characterization of mechanical properties

The preparation of PLA fiber mats with adequate mechanical properties is crucial for their application as medical scaffolds. The mechanical properties of the prepared PLA fiber mat surface areas were analyzed by an advanced AM-FM method in parallel with surface topography measurements [57–59]. This technique was used to investigate the stiffness and the related Young's modulus [60]. Images related to the frequency, stiffness and Young's modulus distribution for individual PLA fibers are shown in Fig. 8. These images clearly show that the surface mechanical properties are dependent on the fiber thickness. The stiffness and Young's modulus of the prepared PLA fiber mats decreased with increasing fiber thickness. The 10% PLA fiber mats

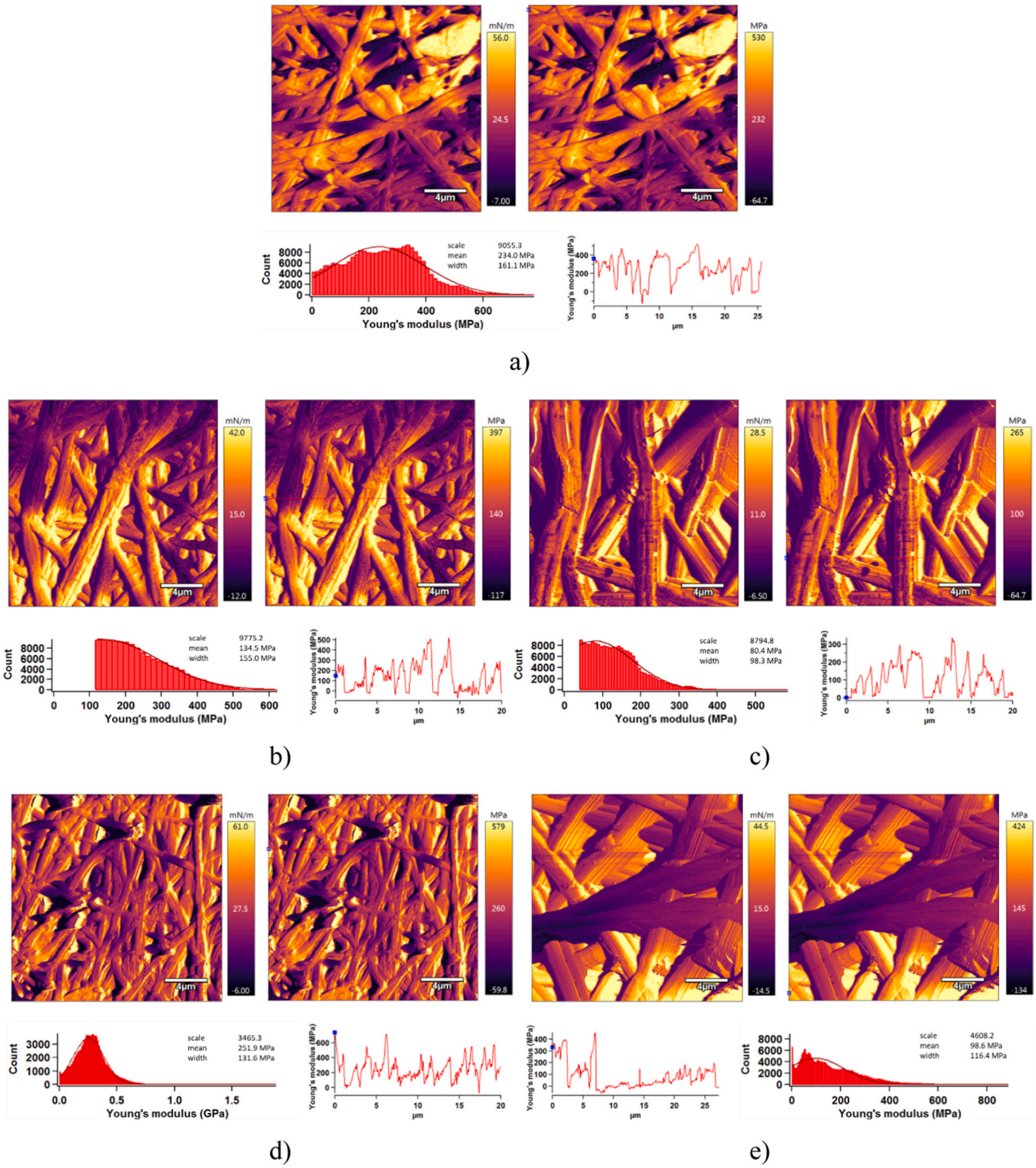

Fig. 8. AM-FM AFM images of PLA fiber mats (from left to right: stiffness, Young's modulus; below: histogram and line profile): a) 3%, b) 5%, c) 7%, d) 10%, e) 12%, f) 10% 30 s plasma treated, g) 10% 60 s plasma treated, h) 10% ASA grafted, i) 10% FA grafted.

achieved the highest value of Young's modulus (251.9 MPa) because they were the thinnest and defect-free. The 30 s plasma treatment time resulted in a slight deterioration in the mechanical properties, while Young's modulus achieved a value 234.5 MPa. The 60 s plasma treatment time led to an additional decrease of Young's modulus, with a value 199.9 MPa, which likely resulted from the degradation process. The PLA fiber mats modified by ASA or FA showed only a slight decrease in the mechanical properties compared with the 30 s plasma-treated PLA samples, while the Young's modulus values were 200.4 MPa and 158.2 MPa, respectively. This could be associated with the formation of thin layers of antimicrobial agent on the PLA fiber mats.

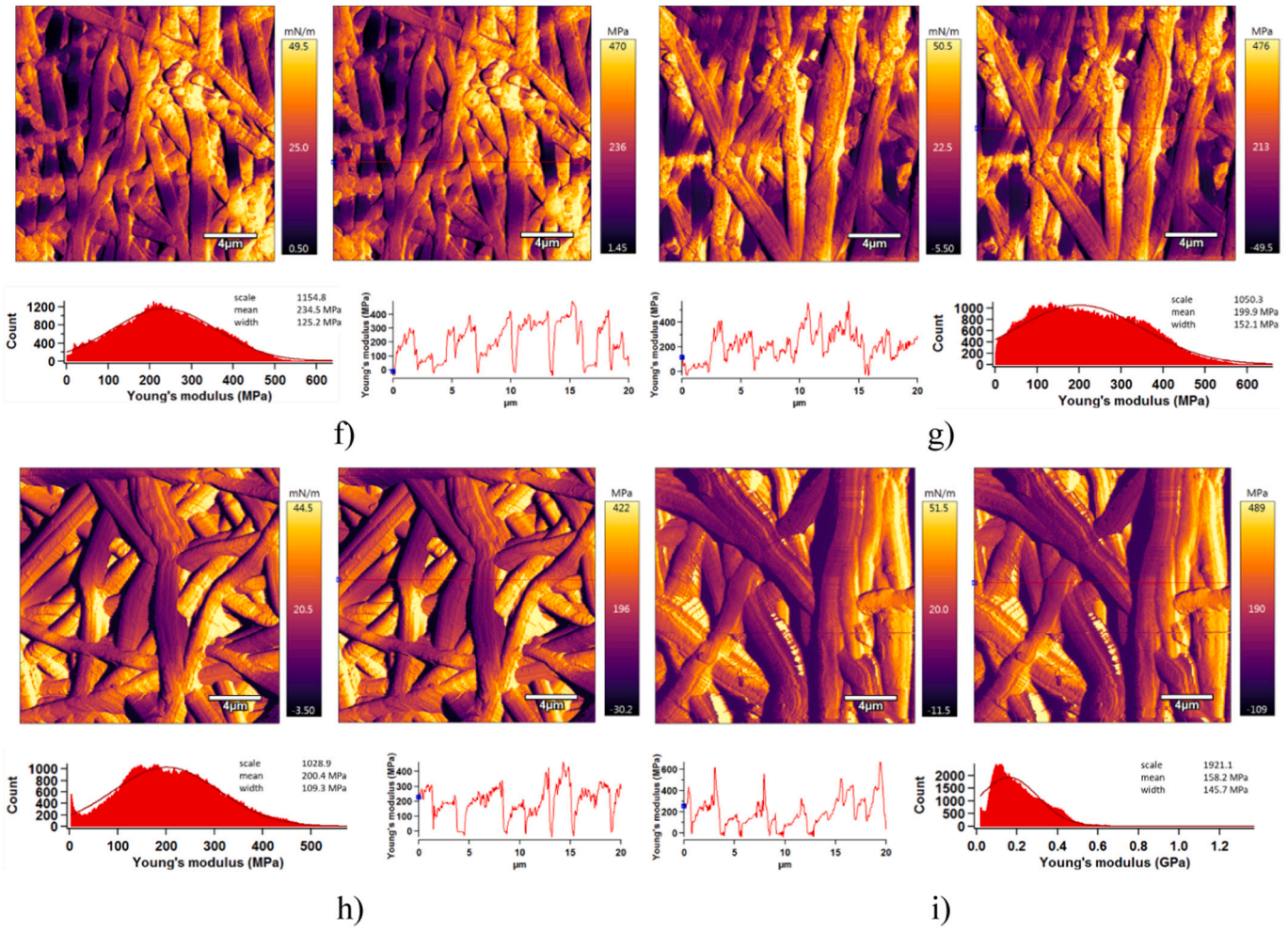

Fig. 8. (*continued*)

3.6. Antibacterial tests

The antimicrobial effect of the PLA samples modified by ASA or FA was investigated using the modified standardized antimicrobial test ISO 22196, which measures the growth inhibition of microorganisms, such as gram-positive *S. aureus* and gram-negative *E. coli*. The antimicrobial activity results are summarized in Table 3, and related images are shown in Fig. S3, Supporting Information. The untreated samples imprinted on the agar showed no bacterial growth inhibition and were overgrown with bacteria after 24 h. This resulted from the poor antimicrobial properties of polymers. Plasma treatment improved the antimicrobial activity of these samples, especially for *S. aureus*. Surface modification by ASA or FA was responsible for the marked antimicrobial activity against *S. aureus* and *E. coli*, with the total inhibition activity reaching 100%. The antimicrobial agents affected the protein in the bacterial cell wall [61] to inhibit the growth of bacteria owing to the instability created in the bacterial cell membranes.

Table 3
Antimicrobial activity.

Sample	Assessment of bacterial colonies[a]	
	S. aureus	*E. coli*
Untreated	5, 5, 4–5	5, 5, 5
Plasma treated	0, 0, 0–1	3–4, 3, 3
ASA grafted	0, 0, 0	0, 0, 0
FA grafted	0, 0, 0	0, 0, 0

[a] The scale for assessing the growth of bacterial colonies: 0 – no growth, 1 – detectable amount (single colony), 2 – detectable amount (combined colony), 3 – second imprint - distinguishable colonies, third imprint can be detected, 4 – third imprint - distinguishable colonies, 5 – overgrown - continuous growth.

4. Conclusion

- PLA fiber mats fabricated through an electrospinning technique were modified with antimicrobial agents by applying plasma treatment to enhance the antimicrobial activity for use in tissue engineering applications. Varying the PLA solution concentration enabled optimization of the electrospinning process.
- PLA fiber mats prepared from a 10% DCM/DMF (70:30) binary PLA solution showed the most suitable surface and mechanical properties.
- The PLA fiber mats were then exposed to low-temperature RF plasma treatment. The treatment time was optimized to achieve maximal reactive centers (hydroperoxides) for subsequent reactions with ASA or FA, which were applied as the antimicrobial agents.
- A plasma treatment time of 30 s was optimal to achieve sufficient wettability and a hydroperoxide concentration.
- The incorporation of ASA or FA into the surface of the PLA fiber mats resulted in enhanced antimicrobial activity against gram-positive *S. aureus* and gram-negative *E. coli* bacteria.

CRediT authorship contribution statement

Anton Popelka: Conceptualization, Methodology, Validation,

Formal analysis, Investigation, Resources, Data curation, Writing - original draft, Writing - review & editing, Visualization, Supervision, Project administration, Funding acquisition. **Asma Abdulkareem**:Investigation, Visualization, Formal analysis. **Abdelrahman A. Mahmoud**: Investigation, Visualization, Formal analysis. **Mohammed J. Naser**: Investigation, Visualization, Formal analysis. **Mahmoud K. Abdelrasool**: Investigation, Visualization, Formal analysis. **Khalid J. Mohamoud**: Investigation, Visualization, Formal analysis. **Mohammed K. Hussein**: Investigation, Visualization, Formal analysis. **Marian Lehocky**: Validation, Resources, Writing - review & editing. **Daniela Vesela**: Investigation, Visualization, Formal analysis. **Petr Humpolíček**:Resources, Validation. **Peter Kasak**: Formal analysis, Visualization, Writing - review & editing.

Declaration of competing interest

The authors declare that they have no known competing financial interests or personal relationships that could have appeared to influence the work reported in this paper.

Acknowledgements

This publication was made possible by UREP grant # 22-076-1-011 from the Qatar National Research Fund (a member of The Qatar Foundation). This publication was supported by the Qatar University Collaborative Grant No. QUCG-CAM-20/21-3. The findings achieved herein are solely the responsibility of the authors. Authors M. L. and P. H. would like to express their gratitude to the Czech Science Foundation (19-16861S) for partial financing of the research. SEM analysis was accomplished in the Central Laboratories unit, Qatar University.

Appendix A. Supplementary data

Supplementary data to this article can be found online at https://doi.org/10.1016/j.surfcoat.2020.126216.

References

[1] F.J. O'Brien, Biomaterials & scaffolds for tissue engineering, Mater. Today 14 (2011) 88–95, https://doi.org/10.1016/S1369-7021(11)70058-X.
[2] S. Khorshidi, A. Solouk, H. Mirzadeh, S. Mazinani, J.M. Lagaron, S. Sharifi, S. Ramakrishna, A review of key challenges of electrospun scaffolds for tissue-engineering applications, J. Tissue Eng. Regen. Med. 10 (2016) 715–738, https://doi.org/10.1002/term.1978.
[3] Y. Wang, H. Guo, D. Ying, Multilayer scaffold of electrospun PLA-PCL-collagen nanofibers as a dural substitute, J. Biomed. Mater. Res. Part B Appl. Biomater. 101 (2013) 1359–1366, https://doi.org/10.1002/jbm.b.32953.
[4] T. Mukai, N. Shirahama, B. Tominaga, K. Ohno, Y. Koyama, K. Takakuda, Development of watertight and bioabsorbable synthetic dural substitutes, Artif. Organs 32 (2008) 473–483, https://doi.org/10.1111/j.1525-1594.2008.00567.x.
[5] C. Kunze, H.E. Bernd, R. Androsch, C. Nischan, T. Freier, S. Kramer, B. Kramp, K.P. Schmitz, In vitro and in vivo studies on blends of isotactic and atactic poly (3-hydroxybutyrate) for development of a dura substitute material, Biomaterials 27 (2006) 192–201, https://doi.org/10.1016/j.biomaterials.2005.05.095.
[6] J. Xie, M.R. MacEwan, W.Z. Ray, W. Liu, D.Y. Siewe, Y. Xia, Radially aligned, electrospun nanofibers as dural substitutes for wound closure and tissue regeneration applications, ACS Nano 4 (2010) 5027–5036, https://doi.org/10.1021/nn101554u.
[7] N. Ohbayashi, T. Inagawa, Y. Katoh, K. Kumano, R. Nagasako, H. Hada, Complication of silastic dural substitute 20 years after dural plasty, Surg. Neurol. 41 (1994) 338–341, https://doi.org/10.1016/0090-3019(94)90187-2.
[8] K. Yamada, S. Miyamoto, M. Takayama, I. Nagata, N. Hashimoto, Y. Ikada, H. Kikuchi, Clinical application of a new bioabsorbable artificial dura mater, J. Neurosurg. 96 (2002) 731–735, https://doi.org/10.3171/jns.2002.96.4.0731.
[9] H.E. Bernd, C. Kunze, T. Freier, K. Sternberg, S. Kramer, D. Behrend, F. Prall, M. Donat, B. Kramp, Poly(3-hydroxybutyrate) (PHB) patches for covering anterior skull base defects an animal study with minipigs, Acta Otolaryngol. 129 (2009) 1010–1017, https://doi.org/10.1080/00016480802552493.
[10] M.J. McClure, D.G. Simpson, G.L. Bowlin, Tri-layered vascular grafts composed of polycaprolactone, elastin, collagen, and silk: optimization of graft properties, J. Mech. Behav. Biomed. Mater. 10 (2012) 48–61, https://doi.org/10.1016/j.jmbbm.2012.02.026.
[11] S. Agarwal, J.H. Wendorff, A. Greiner, Use of electrospinning technique for biomedical applications, Polymer (Guildf) 49 (2008) 5603–5621, https://doi.org/10.1016/j.polymer.2008.09.014.
[12] S. Moon, M. Gil, K.J. Lee, Syringeless electrospinning toward versatile fabrication of nanofiber web, Sci. Rep. 7 (2017) 1–11, https://doi.org/10.1038/srep41424.
[13] D.H. Reneker, A.L. Yarin, Electrospinning jets and polymer nanofibers, Polymer (Guildf) 49 (2008) 2387–2425, https://doi.org/10.1016/j.polymer.2008.02.002.
[14] J. Lannutti, D. Reneker, T. Ma, D. Tomasko, D. Farson, Electrospinning for tissue engineering scaffolds, Mater. Sci. Eng. C 27 (2007) 504–509, https://doi.org/10.1016/j.msec.2006.05.019.
[15] S. Roman, A. Mangera, N.I. Osman, A.J. Bullock, C.R. Chapple, S. Macneil, Developing a tissue engineered repair material for treatment of stress urinary incontinence and pelvic organ prolapse - which cell source? Neurourol. Urodyn. 33 (2014) 531–537, https://doi.org/10.1002/nau.22443.
[16] Y. Chen, L.M. Geever, J.A. Killion, J.G. Lyons, C.L. Higginbotham, D.M. Devine, Review of multifarious applications of poly (lactic acid), Polym.-Plast. Technol. Eng. 55 (2016) 1057–1075, https://doi.org/10.1080/03602559.2015.1132465.
[17] C. Winthrop, New Developments in Polylactic Acid Research, (2014).
[18] I. Novák, A. Popelka, A.S. Luyt, M.M. Chehimi, M. Špírková, I. Janigová, A. Kleinová, P. Stopka, M. Šlouf, V. Vanko, I. Chodák, M. Valentin, Adhesive properties of polyester treated by cold plasma in oxygen and nitrogen atmospheres, Surf. Coat. Technol. 235 (2013) 407–416, https://doi.org/10.1016/j.surfcoat.2013.07.057.
[19] A. Popelka, I. Novák, M.A.S.A. Al-Maadeed, M. Ouederni, I. Krupa, Effect of corona treatment on adhesion enhancement of LLDPE, Surf. Coat. Technol. 335 (2018) 118–125, https://doi.org/10.1016/j.surfcoat.2017.12.018.
[20] T. Jacobs, H. Declercq, N. De Geyter, R. Cornelissen, P. Dubruel, C. Leys, A. Beaurain, E. Payen, R. Morent, Plasma surface modification of polylactic acid to promote interaction with fibroblasts, J. Mater. Sci. Mater. Med. 24 (2013) 469–478, https://doi.org/10.1007/s10856-012-4807-z.
[21] K. Park, J.J. Hyun, J.J. Kim, K.D. Ahn, K.H. Dong, M.J. Young, Acrylic acid-grafted hydrophilic electrospun nanofibrous poly(L-lactic acid) scaffold, Macromol. Res. 14 (2006) 552–558, https://doi.org/10.1007/BF03218723.
[22] G.S. Mann, L.P. Singh, P. Kumar, S. Singh, C. Prakash, On briefing the surface modifications of polylactic acid: a scope for betterment of biomedical structures, J. Thermoplast. Compos. Mater. (2019) 089270571985605, , https://doi.org/10.1177/0892705719856052.
[23] Y. Cheng, S. Deng, P. Chen, R. Ruan, Polylactic acid (PLA) synthesis and modifications: a review, Front. Chem. China 4 (2009) 259–264, https://doi.org/10.1007/s11458-009-0092-x.
[24] T. Bjarnsholt, P.Ø. Jensen, M.J. Fiandaca, J. Pedersen, C.R. Hansen, C.B. Andersen, T. Pressler, M. Givskov, N. Høiby, Pseudomonas aeruginosa biofilms in the respiratory tract of cystic fibrosis patients, Pediatr. Pulmonol. 44 (2009) 547–558, https://doi.org/10.1002/ppul.21011.
[25] W. Costerton, R. Veeh, M. Shirtliff, M. Pasmore, C. Post, G. Ehrlich, The application of biofilm science to the study and control of chronic bacterial infections, J. Clin. Invest. 112 (2003) 1466–1477, https://doi.org/10.1172/jci20365.
[26] M.C. Robson, Wound infection. A failure of wound healing caused by an imbalance of bacteria, Surg. Clin. North Am. 77 (1997) 637–650, https://doi.org/10.1016/s0039-6109(05)70572-7.
[27] K.P. Houglum, D.A. Brenner, M. Chojkier, Ascorbic acid stimulation of collagen biosynthesis independent of hydroxylation, Am. J. Clin. Nutr. 54 (1991) 1141S–1143S, https://doi.org/10.1093/ajcn/54.6.1141s.
[28] R.K. Das, S.K. Brar, M. Verma, Recent advances in the biomedical applications of fumaric acid and its ester derivatives: the multifaceted alternative therapeutics, Pharmacol. Rep. 68 (2016) 404–414, https://doi.org/10.1016/j.pharep.2015.10.007.
[29] M. Turalija, S. Bischof, A. Budimir, S. Gaan, Antimicrobial PLA films from environment friendly additives, Compos. Part B Eng. 102 (2016) 94–99, https://doi.org/10.1016/j.compositesb.2016.07.017.
[30] Y. Qi, H.L. Ma, Z.H. Du, B. Yang, J. Wu, R. Wang, X.Q. Zhang, Hydrophilic and antibacterial modification of poly(lactic acid) films by γ-ray irradiation, ACS Omega 4 (2019) 21439–21445, https://doi.org/10.1021/acsomega.9b03132.
[31] I.S.M.A. Tawakkal, M.J. Cran, J. Miltz, S.W. Bigger, A review of poly(lactic acid)-based materials for antimicrobial packaging, J. Food Sci. 79 (2014) R1477–R1490, https://doi.org/10.1111/1750-3841.12534.
[32] M.H. Kudzin, Z. Mrozińska, Biofunctionalization of textile materials. 2. Antimicrobial modification of poly(lactide) (PLA) nonwoven fabrics by fosfomycin, Polymers (Basel) 12 (2020) 768, https://doi.org/10.3390/polym12040768.
[33] A. H, Ascorbic acid (vitamin C), Nature 134 (1934) 724–725, https://doi.org/10.1038/134724a0.
[34] H. Chang Liang, F. Ben Dong, S. Hai Qing, J. Xiao Lin, W. Xu Bin, Fumaric acid, an antibacterial component of Aloe vera L, Afr. J. Biotechnol. 10 (2011) 2973–2977, https://doi.org/10.5897/ajb10.1497.
[35] C.D. Wagner, R.H. Smith, E.D. Peters, Determination of organic peroxides: evaluation of modified iodometric method, Anal. Chem. 19 (1947) 976–979, https://doi.org/10.1021/ac60012a010.
[36] ISO - ISO 22196:2011 - measurement of antibacterial activity on plastics and other non-porous surfaces, (n.d.). https://www.iso.org/standard/54431.html (accessed July 7, 2020).
[37] R. Casasola, N.L. Thomas, A. Trybala, S. Georgiadou, Electrospun poly lactic acid (PLA) fibres: effect of different solvent systems on fibre morphology and diameter, Polymer (Guildf) 55 (2014) 4728–4737, https://doi.org/10.1016/j.polymer.2014.06.032.
[38] A.B.D. Cassie, S. Baxter, Wettability of porous surfaces, Trans. Faraday Soc. 40 (1944) 546–551, https://doi.org/10.1039/tf9444000546.

[39] M. Zhu, W. Zuo, H. Yu, W. Yang, Y. Chen, Superhydrophobic surface directly created by electrospinning based on hydrophilic material, J. Mater. Sci. 41 (2006) 3793–3797, https://doi.org/10.1007/s10853-005-5910-z.
[40] K. Acatay, E. Simsek, C. Ow-Yang, Y.Z. Menceloglu, Tunable, superhydrophobically stable polymeric surfaces by electrospinning, Angew. Chem. Int. Ed. 43 (2004) 5210–5213, https://doi.org/10.1002/anie.200461092.
[41] M. Ma, Y. Mao, M. Gupta, K.K. Gleason, G.C. Rutledge, Superhydrophobic fabrics produced by electrospinning and chemical vapor deposition, Macromolecules 38 (2005) 9742–9748, https://doi.org/10.1021/ma0511189.
[42] S.T. Yohe, J.D. Freedman, E.J. Falde, Y.L. Colson, M.W. Grinstaff, A mechanistic study of wetting superhydrophobic porous 3D meshes, Adv. Funct. Mater. 23 (2013) 3628–3637, https://doi.org/10.1002/adfm.201203111.
[43] W. Cui, X. Li, S. Zhou, J. Weng, Degradation patterns and surface wettability of electrospun fibrous mats, Polym. Degrad. Stab. 93 (2008) 731–738, https://doi.org/10.1016/j.polymdegradstab. 2007.12.002.
[44] O. Koysuren, H.N. Koysuren, Characterization of poly(methyl methacrylate) nanofiber mats by electrospinning process, J. Macromol. Sci. Part A Pure Appl. Chem. 53 (2016) 691–698, https://doi.org/10.1080/10601325.2016.1224627.
[45] P. Sadeghi, H. Tavanai, A. Khoddami, Hydrophobicity of fluorocarbon-finished electrospun poly (acrylonitrile) nanofibrous webs, J. Text. Inst. 108 (2017) 189–195, https://doi.org/10.1080/00405000.2016.1160812.
[46] P.K. Szewczyk, D.P. Ura, S. Metwally, J. Knapczyk-Korczak, M. Gajek, M.M. Marzec, A. Bernasik, U. Stachewicz, Roughness and fiber fraction dominated wetting of electrospun fiber-based porous meshes, Polymers (Basel) 11 (2018), https://doi.org/10.3390/polym11010034.
[47] R.M. Rasal, A.V. Janorkar, D.E. Hirt, Poly(lactic acid) modifications, Prog. Polym. Sci. 35 (2010) 338–356, https://doi.org/10.1016/j.progpolymsci.2009.12.003.
[48] C. Lambaré, P.Y. Tessier, F. Poncin-Epaillard, D. Debarnot, Plasma functionalization and etching for enhancing metal adhesion onto polymeric substrates, RSC Adv. 5 (2015) 62348–62357, https://doi.org/10.1039/c5ra08844e.
[49] R.N. Wenzel, Resistance of solid surfaces to wetting by water, Ind. Eng. Chem. 28 (1936) 988–994, https://doi.org/10.1021/ie50320a024.
[50] E. Niki, Action of ascorbic acid as a scavenger of active and stable oxygen radicals, Am. J. Clin. Nutr. 54 (1991) 1119S–1124S https://academic.oup.com/ajcn/article-abstract/54/6/1119S/4715143?redirectedFrom=fulltext , Accessed date: 22 April 2020.
[51] T.E.A. Ardjani, J.R. Alvarez-Idaboy, Radical scavenging activity of ascorbic acid analogs: kinetics and mechanisms, Theor. Chem. Accounts 137 (2018) 1–8, https://doi.org/10.1007/s00214-018-2252-x.
[52] A. Popelka, P.N. Khanam, M.A. AlMaadeed, Surface modification of polyethylene/graphene composite using corona discharge, J. Phys. D. Appl. Phys. 51 (2018) 105302, , https://doi.org/10.1088/1361-6463/AAA9D6.
[53] NPCS Board of Consultants and Engineers, The Complete Book on Adhesives, Glues & Resins Technology (with Process & Formulations), (2016).
[54] E. Meaurio, N. López-Rodríguez, J.R. Sarasua, Infrared spectrum of poly(L-lactide): application to crystallinity studies, Macromolecules 39 (2006) 9291–9301, https://doi.org/10.1021/ma061890r.
[55] R. Nyquist, Anhydrides, Interpret. Infrared, Raman, Nucl. Magn. Reson. Spectra, (2001), pp. 205–212, https://doi.org/10.1016/b978-012523475-7/50175-3.
[56] B. Hergelová, A. Zahoranová, D. Kováčik, M. Stupavská, M. Černák, Polylactic acid surface activation by atmospheric pressure dielectric barrier discharge plasma, Open Chem. 13 (2015) 564–569, https://doi.org/10.1515/chem-2015-0067.
[57] G. Lamour, C.K. Yip, H. Li, J. Gsponer, High intrinsic mechanical flexibility of mouse prion nanofibrils revealed by measurements of axial and radial young's moduli, ACS Nano 8 (2014) 3851–3861, https://doi.org/10.1021/nn5007013.
[58] Z.N. Mahani, M. Tajvidi, Viscoelastic mapping of spruce-polyurethane bond line area using AM-FM atomic force microscopy, Int. J. Adhes. Adhes. 79 (2017) 59–66, https://doi.org/10.1016/j.ijadhadh.2017.09.005.
[59] K.E. Strawhecker, E.J. Sandoz-Rosado, T.A. Stockdale, E.D. Laird, Background data for modulus mapping high-performance polyethylene fiber morphologies, Data Br 10 (2017) 413–420, https://doi.org/10.1016/j.dib.2016.11.071.
[60] A. Antunes, A. Popelka, O. Aljarod, M.K. Hassan, A.S. Luyt, Effects of rutile-TiO2 nanoparticles on accelerated weathering degradation of poly(lactic acid), Polymers (Basel) 12 (2020), https://doi.org/10.3390/POLYM12051096.
[61] J.M. Jay, Modern Food Microbiology, Springer US, Boston, MA, 1992, https://doi.org/10.1007/978-94-011-6480-1.